Additive Photonic Colors in the Brazilian Diamond Weevil, Entimus imperialis

Mouchet, Sébastien; Vigneron, Jean-Pol; Colomer, Jean-François; Vandenbem, Cedric; Deparis, Olivier

Published in:
Proceedings of SPIE - The International Society for Optical Engineering

DOI:
10.1117/12.928352

Publication date:
2012

Document Version
Publisher's PDF, also known as Version of record

Additive Photonic Colors in the Brazilian Diamond Weevil, *Entimus imperialis*

S. Mouchet[a,*], J.-P. Vigneron[a], J.-F. Colomer[a], C. Vandenbem[a], O. Deparis[a]

[a] Solid-State Physics Laboratory, Facultés Universitaires Notre-Dame de la Paix (FUNDP), Rue de Bruxelles 61, B-5000, Namur, Belgium

ABSTRACT

Structurally colored nano-architectures found in living organisms are complex optical materials, giving rise to multi-scale visual effects. In arthropods, these structures often consist of porous biopolymers and form natural photonic crystals. A signature of the structural origin of coloration in insects is iridescence, i.e., color changes with the viewing angle. In the scales located on the elytra of the Brazilian weevil *Entimus imperialis* (Curculionidae), three-dimensional photonic crystals are observed. On one hand, each of them interacts independently with light, producing a single color which is observed by optical microscopy and ranges from blue to orange. On the other hand, the color perceived by the naked eye is due to multi-length-scale light effects involving different orientations of a single photonic crystal. This disorder in crystal orientations alters the light propagation in such a way that the crystal iridescence is removed. *Entimus imperialis* is therefore a remarkable example of additive photonic colors produced by a complex multi-scale organic architecture. In order to study this specific natural photonic structure, electron microscopy is used. The structure turns out to be formed of a single type of photonic crystal with different orientations within each scale on the elytra. Our modeling approach takes into account the disorder in the photonic crystals and explains why the structure displays bright colors at the level of individual scales and a non-iridescent green color in the far-field.

Keywords: Beetle scale, natural photonic crystals, photonic bandgap materials, structural color, iridescence, Coleoptera, nanoarchitecture, bioinspiration, biomimetics, biomaterials

1. INTRODUCTION

For centuries, humans have been interested in colors and in their production methods in order to use them in different fields, e.g., painting, textile dye, ceramics decoration, food coloring… or by simple wish to understand phenomena such as the yellowing of tree leaves, the color changes at sunset, the white coloration of clouds, the colors of rainbows, those of *aurora borealis* and *australis*…

Colors are generally divided into two categories according to their origin: pigmentary colors, due to selective absorption of incident light by a pigment, and structural colors, due to the interplay of light with physical nanostructures. In living organisms, colors are produced by one of these two mechanisms or both simultaneously. The animal kingdom widely uses physical colors in order to display surprising color effects.[1, 2] It is the case for numerous butterflies, beetles, birds, fishes… The structures at the origin of their colors were optimized for more than 500 million years. Photonic crystals which are studied in this paper are one example of structural colors found in nature. They consist in media composed of a periodic distribution of materials with different refractive indices. The periodicity of the dielectric permittivity influences light propagation. In the case of insects, the building materials are mainly air and a biopolymer: chitin $(C_8H_{13}O_5N)_n$. These photonic structures are highly ordered and extremely sophisticated porous materials. Their structures can be very complex leading to remarkable coloration effects. Furthermore, these nanostructures which are a source of inspiration for humans through a biomimetic approach can have other interesting properties such as a hygrochromic behavior[3-8] (the ability to change coloration when soaked in water), gas or vapor sensing,[9-11] antireflection property,[12] light absorption[13]…

* Email: sebastien.mouchet@fundp.ac.be; phone: +32 (0)81 724701; fax: +32 (0)81 724707

The Nature of Light: Light in Nature IV, edited by Rongguang Liang, Proc. of SPIE Vol. 8480
848003 · © 2012 SPIE · CCC code: 0277-786/12/$18 · doi: 10.1117/12.928352

In this paper, we investigated the diamond weevil, *Entimus imperialis* (Curculionidae - Forster 1771). This beetle is a Brazilian weevil whose size reaches approximately 3 cm (fig. 1). It is a very common insect in Brazil where it lives mainly on tree leaves. This beetle exhibits green spots on its elytra. The origin of this coloration is physical despite the fact that it is not iridescent, as many physical structures. For a long time, it had been used as decoration by several Amazonian populations and nowadays it is used in jewellery with other materials such as gold.

Figure 1. Photograph of the Brazilian weevil *Entimus imperialis*. (colors available online)

This beetle has already been studied previously,[14] but this article consists in a deeper study of the light interaction with the photonic nanostructures. We demonstrate here that the color of the weevil is due to the presence of three-dimensional photonic crystals and for this purpose we used optical and electron microscopies, spectrophotometry (SP), microspectrophotometry (MSP), photonic band structure calculations, and simulations of reflectance spectra by Rigorous Coupled Wave Analysis (RCWA)[15, 16]. We also assess the diffraction properties of the photonic structure found on its cuticle.

This beetle is an astonishing example of additive photonic colors produced by complex multi-length-scale organic structures: the weevil color is produced by a disordered set of ordered photonic crystals. Each crystal reflects light independently, giving rise to single bright colors ranging from blue to orange (as observed by optical microscopy), while the color perceived by human eye in the far-field is matt green. The interaction of light with distinct orientations of the photonic crystal at different length scales alters these colors in such a way that a non-iridescent coloration is exhibited.

2. METHODOLOGY

2.1 Samples

We obtained samples from a commercial insect supplier, who identified them to species level as *Entimus imperialis*. They were caught in the municipality of Linhares in the State of Espírito Santo in January 1983. This long period between capture and observations had no major consequence on the coloration of these insects. This fact calls for the structural origin of the coloration of these Curculionidae. Pigmentary colors would indeed have bleached by ultraviolet rays since then.

2.2 Morphological and optical characterizations

In order to get a deep understanding of the complex behavior of natural photonic nanostructures, it is essential to realize morphological and optical characterizations. In spite of the fact that microscopy provided us with a two-dimensional image from a three-dimensional structure, it allowed us however to describe precisely the photonic structure at the origin of the coloration. For microscopy observations, we used an Olympus BX61 optical microscope equipped with an

Olympus XC50 camera and an Olympus BX-UCB lamp as well as a Field Emission Scanning Electron Microscope JEOL-7500F. In the latter case, samples whose sizes were typically $5 \times 5\ \mathrm{mm}^2$ were coated by a 25 nm-gold layer.

In order to get a quantitative description of the colors produced by the nanostructures, it is mandatory to resort to spectrophotometry (SP). Reflectance spectra were measured thanks to an Avantes AvaSpec-2048-2 spectrophotometer and an Avantes AvaLight-DH-S-BAL deuterium/halogen light source. The measurements were realized in specular configuration, i.e., the absolute incidence and detection angles were equal. The spot size of the incidence beam on the sample was several square millimeters. We note that the measured quantity was the reflection factor and not the reflectance. In this paper, the reflection factor R is defined as the ratio between the reflected intensity I and a reference intensity W with a correction factor B taking into account the noise due to light rays coming from other sources than the lamp used for the measurements:

$$R = \frac{I-B}{W-B}. \tag{1}$$

The reference intensity W was acquired using a white reference standard Avantes WS-2 based on PTFE. The reflection factor of some samples, reflecting light very directionally, can exceed 100% at some wavelengths. We have to be especially careful when using reference standard because the results can vary according to this standard.

Reflectance spectra of well defined zones on the samples were recorded using a microspectrophotometer (MSP). The set-up was mainly composed of an optical microscope linked to an Avantes AvaSpec-2048-2 spectrophotometer. A halogen light source illuminated the beetle elytra at an incidence angle of about 40° with respect to the normal to the sample. Like in SP measurements, the reflection factor was in fact measured. The typical size of the illuminated spots was smaller than $1500\ \mu\mathrm{m}^2$.

2.3 Dominant wavelength estimation

The dominant wavelength formula provides us with an estimate of the position of the peak in the reflectance spectrum of a multilayered structure as soon as the layer thicknesses and their refractive indices are known.[16-18] Because of the periodicity of the multilayer, light cannot actually propagate at some wavelengths inside the material. If the incidence angle (with respect to the normal to the multilayer) is θ and n_0 is the incidence medium refractive index, then the position of the reflectance maximum λ is given by:

$$\lambda = \frac{2a\sqrt{\bar{n}^2 - n_0^2 \sin^2\theta}}{m} \tag{2}$$

where a is the period, $\bar{n}$ is the effective refractive index of the multilayer and m is an integer whose value is determined so that the dominant wavelength belongs to the visible part of the electromagnetic spectrum. For natural photonic structure, this value is generally equal to $m = 1$. This formula is valid for weak refractive index contrasts and for wavelengths relatively longer than the period a.

By calculating an effective refractive index, the multilayer is approximated by a homogenous effective medium. We can estimate the average refractive index $\bar{n}$ using the rules of capacitances[17] which is based on the calculation of the weighted averages of the dielectric constants found in the medium. The weights depend on the relative volumes of the different materials composing the photonic structure.

At normal incidence ($\theta = 0°$), the dominant reflected wavelength can be estimated using:

$$\lambda = \frac{2a\bar{n}}{m}. \tag{3}$$

A two- or three-dimensional photonic crystal can be approximated by a multilayered medium depending on the orientation of the crystal[16, 18]. When light illuminates such a crystal, it can indeed be viewed as a periodic stacking of homogenous layers. According to its orientation, the photonic crystal will be assimilated to a specific multilayer.[16] In the same way it is applied for multilayered reflectors, an average refractive index $\bar{n}$ of a homogenous effective medium can be calculated using the rules of capacitances[17] as well. The dominant wavelength λ reflected by the photonic crystal can be estimated using the following formula[16, 18]:

$$\lambda = \frac{2p\bar{n}}{m} \quad (4)$$

where p is the distance between two parallel reticular planes corresponding to a given orientation and replace here the multilayer period a. We note that this formula is only valid in a normal incidence configuration.

2.4 Numerical computation aspects

Dominant wavelength calculations provide us with a first clue regarding the reflected color without any more details. In order to realize a rigorous study of natural photonic crystals, it is necessary to combine experimental characterizations with numerical predictions. These predictions based on a photonic model of the structure have to be compared with SP measurements.

In our numerical study, we calculated the reflectance spectra of the photonic structure model by Rigorous Coupled Wave Analysis (RCWA) method, which solves exactly the Maxwell's equations governing light propagation in optically inhomogeneous media.[15, 16] This computational method was used for the assessment of the diffraction properties of the photonic crystal and the calculation of total reflectance spectra. At least 8×8 plane waves were needed in Fourier series expansion of the spatially varying dielectric constant in order to achieve numerical convergence.

The photonic band structure of the idealized photonic crystal was calculated using the MIT Photonic-Bands package (MPB)[19] with $64 \times 64 \times 64$ plane waves.The calculated band gaps corresponded to reflected wavelengths.

2.5 Chromaticity diagram

Since the description of a color cannot be restricted to its reflectance spectrum, we decided to use the chromaticity diagram defined by the *Commission Internationale de l'Eclairage* (CIE) in 1931 according to a method developed elsewhere.[17] In this representation, colors perceived by the human eye are quantified using reflectance spectra and presented on a 2-degree observer chromaticity diagram.[20, 21] The two independent coordinates (x, y) are called chromaticity coordinates. We note that this diagram is only valid for representing the colors perceived by human eyes but not by other animals.

3. RESULTS AND DISCUSSION

3.1 Morphology

In spite of the fact that *Entimus imperialis* exhibits dull green spots when seen at long distance, observations made by optical microscope reveal flat and elongated scales with shiny colors on its cuticle (fig. 2a-d). The scales are also observed with the electron microscope at higher magnification (fig. 3a-b). These scales are gathered in sets around cavities (fig. 2b) forming rows (fig. 2a). The average length of the scales is 100 µm (± 15 µm) while the width at half-length is 50 µm (± 5 µm) and the thickness 2200 nm (± 250 nm). They reflect strongly light at specific wavelengths giving rise to various colors ranging from blue to orange (fig. 2b-d). One single scale is often divided into a few photonic domains differing by their colors (fig. 2c). The size of these domains is typically 30 or 40 µm. We note that the thorax and legs are also covered with such shiny scales.

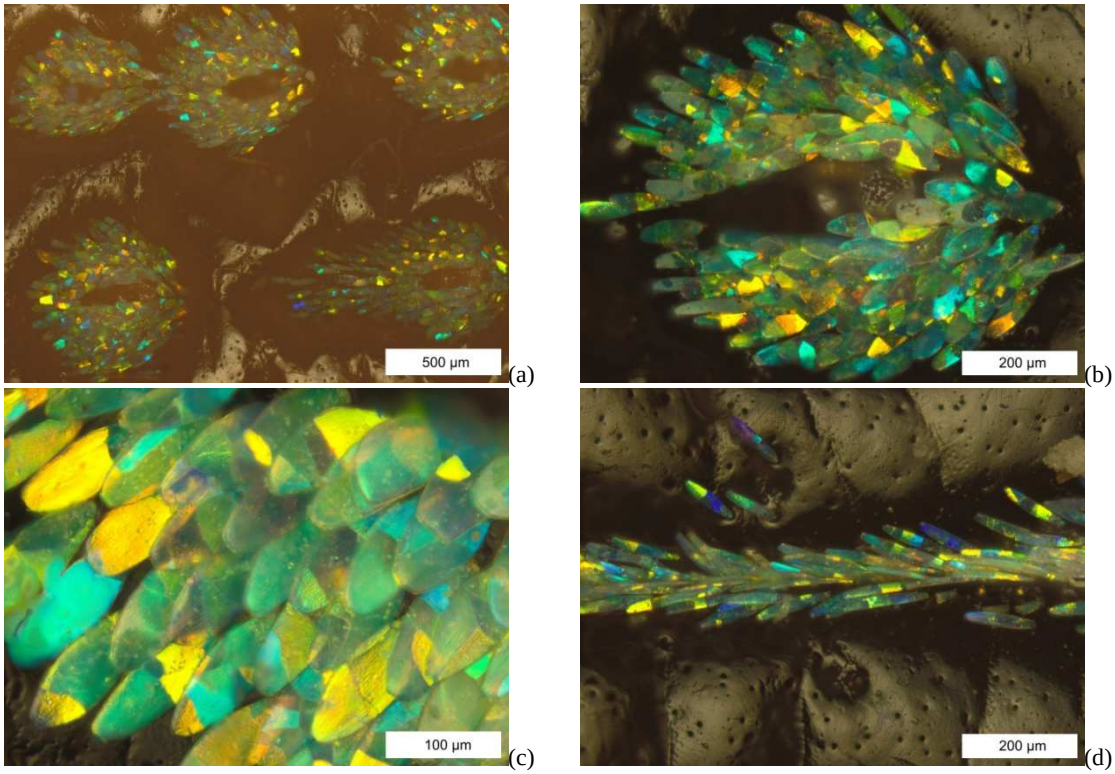

Figure 2. Optical micrographs of the cuticle surface. Scales reflect many colors, ranging from blue to orange. Each scale is made up of several photonic crystal domains. (a) Two rows of scales. (b) Scales gathered around a cavity. (c) Enlarged view of the scales in (b). (d) Junction between the two elytra. (colors available online)

Images obtained by electron microscopy show the photonic nanostructure inside the outer shell of the scales (fig. 3c-f). It consists in a three-dimensional photonic crystal made of thin chitin layers with a two-dimensional triangular lattice of cylindrical perforations (average diameter: 135 ± 14 nm) on which a two-dimensional triangular lattice of cylindrical protrusions (average diameter: 160 ± 15 nm) is found. The height of these protrusions is 150 nm (± 25 nm). The distance a between the centers of two neighboring perforations is 280 ± 10 nm. The chitin layer thickness is 79 nm. This structure is similar to the one found on the cuticle of *Pachyrrhynchus congestus pavonius* (Heller 1921),[18] a weevil from Philippines, characterized by orange circular rings on the dorsal and ventral side of the thorax and abdomen. Here, the photonic polycrystal is, however, made of photonic crystal grains which are larger than the ones found in *Pachyrrhynchus congestus pavonius*.

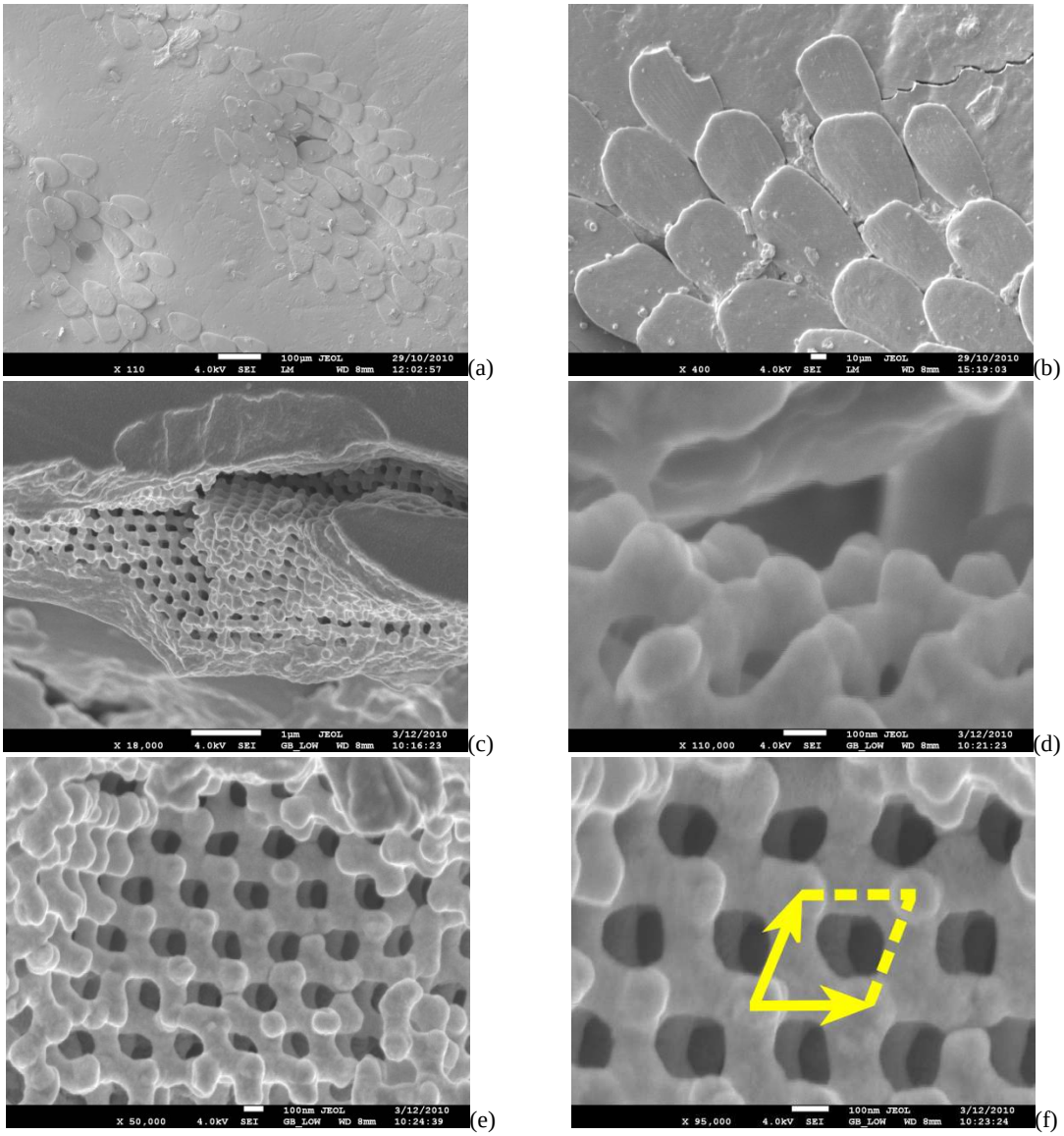

Figure 3. Electron micrographs of the scales. (a) Two rows of scales. (b) Enlarged view of the scales in (a). (c-f) Electron micrographs of broken scales showing the inner nanostructure of the photonic crystal. It is made of chitin layers with cylindrical perforations and protrusions arranged according to a two-dimensional triangular lattice. The two basis vectors of the unit cell which are parallel to the chitin layers are drawn in yellow (f). (colors available online)

The unit cell of the photonic crystal contains three sites: one protrusion, one empty site and one perforation (fig. 4). The size of the unit cell is of the order of visible light wavelengths.

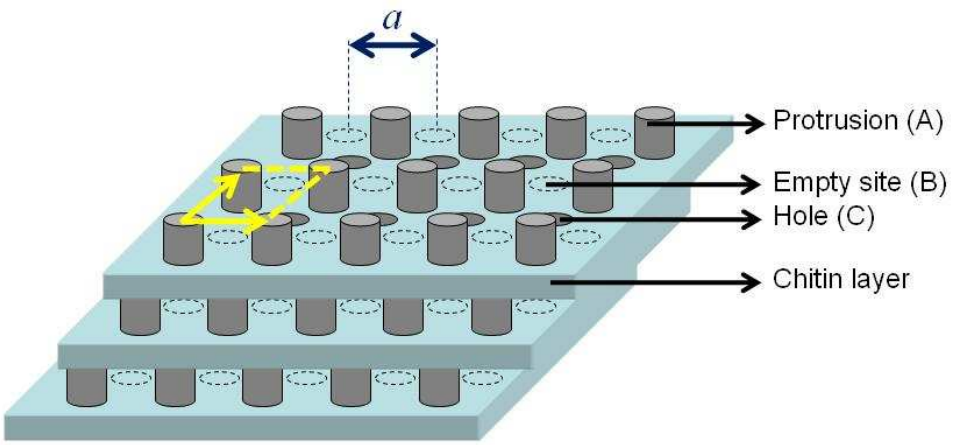

Figure 4. Schematic view of the photonic crystal. It consists in a stack of perforated chitin layers covered by cylindrical protrusions. The unit cell is made up of one protrusion (A) spacing the chitin layers, one empty site (B) and one perforation (C). An ABC stacking of these chitin layers leads to a face-centered cubic (FCC) structure. The two basis vectors of the unit cell which are parallel to the chitin layer are drawn in yellow. (colors available online)

Analyzing the possible stacking schemes on the basis of electron micrographs following the same method as described elsewhere,[18] we determined that the stacking of the chitin layers in each photonic domain of the polycrystal forms a face-centered cubic structure (fig. 5). Protrusions (A), empty sites (B) and perforations (C) are vertically aligned and repeated in that order leading to an ABC stack. Each photonic crystal grain is iridescent giving rise to very different reflected colors depending on the orientation of the crystal. Using the relation $d = \sqrt{2}a$ between the length d of a cube edge and the distance a between two neighboring perforation centers (determined from electron microscopy images), we evaluated the crystal parameter d to be 396 nm.

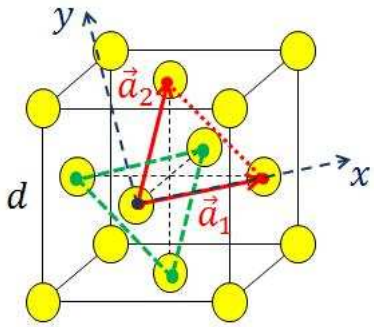

Figure 5. Orientation of two basis vectors of the unit cell (parallel to the chitin layer) in the FCC lattice. Two reticular planes are highlighted in green and red. The norm a of vectors $\vec{a}_1$ and $\vec{a}_2$ is equal to the distance between two neighboring perforation centers. (colors available online)

3.2 Reflectance

Orientational disorder in the photonic polycrystals eliminates the iridescence effect. In order to highlight this behavior, reflectance spectra were acquired from different photonic crystal domains using MSP (fig. 6a). The size of the analyzed zones was smaller than 1500 μm^2, i.e., of the order of the size of the photonic crystal domains. Reflectance peaks are observed at very various wavelengths according to the position on the scale. These peaks correspond to the different colors observed by optical microscopy (fig. 2) and are due to the selective reflection on the photonic crystals. Reflectance spectra acquired by SP (fig. 6b) at different incidence and reflection angles in a specular configuration do not present the characteristic iridescence shift, as in the case of many other natural photonic nanostructures.[2, 22, 23] These spectra differ from those obtained by MSP. They were measured from a defined zone of the samples whose size was

equal to a few millimeters. As we will see, they can be seen as the result of an average of the spectra measured on single photonic crystal domains by to MSP.

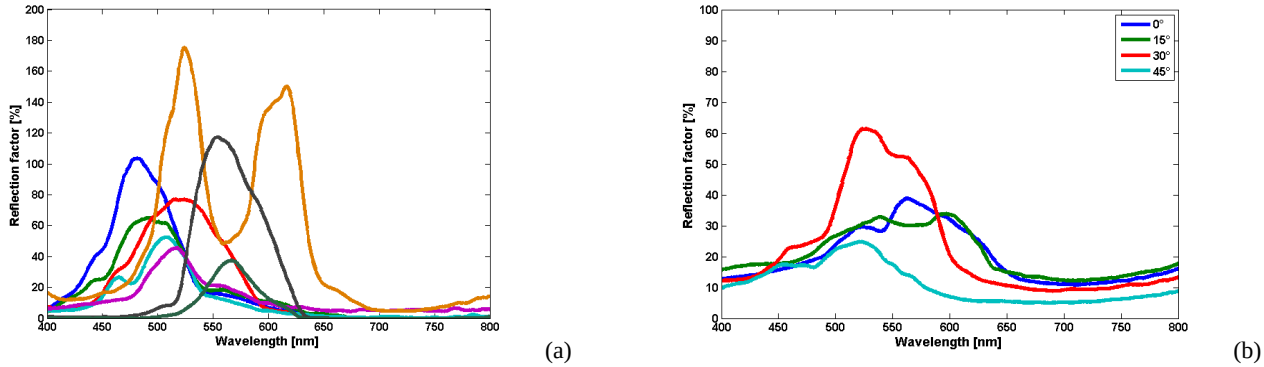

(a) (b)

Figure 6. (a) Reflectance spectra corresponding to different photonic crystal domains measured by microspectrophotometry. The orange curve is due to a measurement made on two neighboring photonic domains with different orientations. (b) Reflectance spectra obtained by spectrophotometry at different incidence and reflection angles (measured with respect to the normal to the cuticle) in specular configuration. (colors available online)

3.3 Theoretical predictions and numerical simulations

In spite of the fact that the photonic nanostructure is polycrystalline, i.e., one single scale is made of the same crystal with different orientations, we first consider the case of a crystal having one unique orientation. Since the size of the photonic crystal domains is several tens of microns, the study of one single orientation is relevant, with respect to e.g., MSP measurements.

Photonic band structure was calculated using MPB software[19] (fig. 7). Of course, the refractive index contrast due to air and chitin is too small to generate complete band gaps. However, partial band gaps observed in this diagram correspond to the reflected wavelengths for a range of wavevector directions. Incident waves with wavelengths of 577, 506, 472 and 487 nm cannot propagate in the photonic crystal according to ΓL, ΓX, WK and ΓK directions, respectively, and are therefore reflected by the crystal. These wavelengths correspond to some of the peak positions measured by MSP (fig. 6a). The structure observed by electron microscopy is therefore at the origin of the colorations of the diamond weevil.

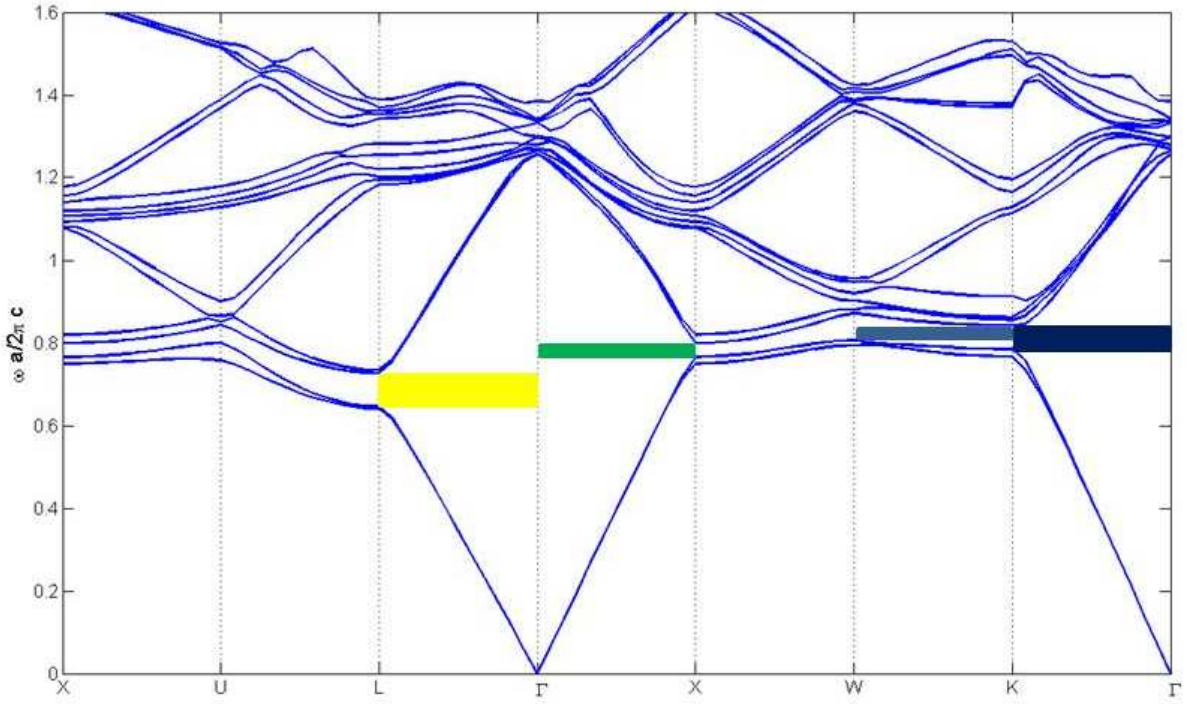

Figure 7. Photonic band structure of the crystal found in the scales of *Entimus imperialis*. Partial band gaps are highlighted by color rectangles. (colors available online)

Approximating the three-dimensional photonic crystal by a homogenous effective medium and applying eq. (3), we can easily estimate the dominant wavelengths reflected in the ΓL, ΓX and ΓK directions which correspond to the (111), (100) and (110) directions in the direct space, respectively. Assuming a structure made of air ($n_{\text{air}} = 1$) and chitin ($n_{\text{chitin}} = 1.56$ [24]) with a filling factor f (ratio between the chitin volume V_{chitin} in the unit cell and the total unit cell volume V_c, calculated from electron micrographs) equal to $f = V_{chitin}/V_c = 0.47$, we evaluated the effective refractive index $\bar{n}$ to be 1.23.

In the case of the (111) direction, the p parameter (eq. 4) is equal to the third of the diagonal of the cube (fig. 5)[†], $p = d\sqrt{3}/3 = a\sqrt{2/3} = 229$ nm and the dominant reflected wavelength is therefore equal to $\lambda = 2 \times 229 \times 1.23/1 = 563$ nm.

Applying this approximation to the (100) direction, p is now equal to the half of the cube edge d, $p = d/2 = a/\sqrt{2} = 198$ nm and the dominant reflected wavelength is equal to $\lambda = 2 \times 198 \times 1.23/1 = 487$ nm .

In the case of the (110) direction, the distance between two reticular planes is $p = d\sqrt{2}/3 = 2a/3 = 187$ nm and the dominant reflected wavelength is $\lambda = 2 \times 187 \times 1.23/1 = 459$ nm.

According to the orientation of the photonic nanostructure, crystal facets with different Miller indices are exhibited on the scale surfaces. As we can deduce from the photonic band structure, the reflectance spectrum varies according to the crystal facet. Using RCWA, we calculated reflectance spectra corresponding to the (111) direction at different incidence angles θ (fig. 8). At normal incidence, the main peak is positioned at 578 nm. This is perfectly in accordance with the wavelength predicted from the photonic band structure. Other peaks are located at 288 and 304 nm. The

[†] This value is obtained by considering a FCC symmetry of the photonic crystal. We note that we can also obtain the parameter p (equal to the distance between chitin layers) by summing the chitin layer thickness and the protrusion height.[18] Accordingly, $p = 79 + 150 = 229$ nm, which is exactly equal to the third of the cube diagonal. This result confirms in fact the FCC symmetry of the photonic crystal.

dominant wavelength approximation shows us that these peaks correspond to the $m = 2$ harmonics $\lambda = 2p\bar{n}/m = 2 \times 229 \times 1.23/2 = 282$ nm. The blue shift of the reflectance spectrum with increasing incidence angles, also predicted by eq. (2) is observed (fig. 8).

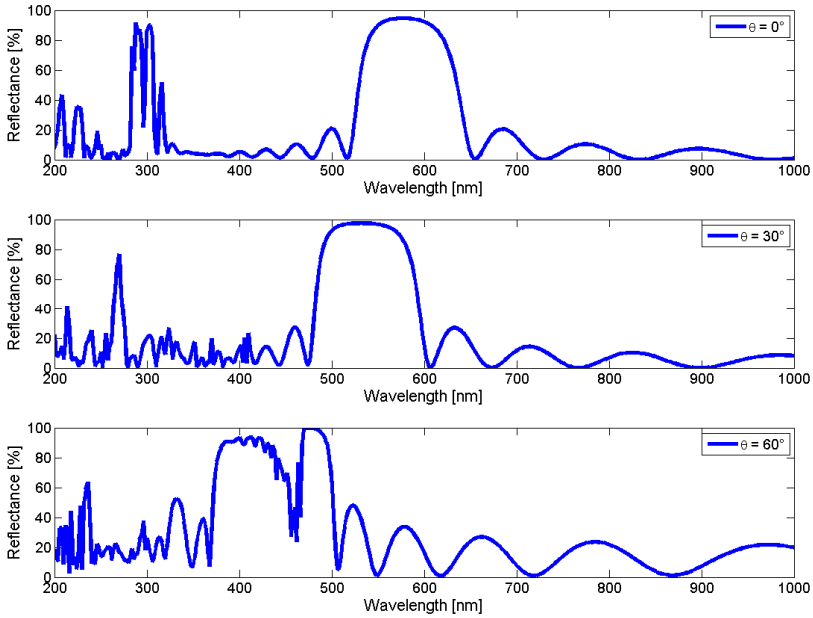

Figure 8. Reflectance spectra calculated for the (111) direction of the photonic crystal at incidence angles θ equal to 0°, 30° and 60° (from top graph to bottom graph).

The peak positions determined by the photonic band structure, approximation of the dominant wavelength, RCWA and MSP are all in good agreement (table 1). We note that the greater difference at short wavelengths is explained by the fact that the calculation of the effective refractive index $\bar{n}$ is valid at long wavelengths. The related colors are yellow, green and blue, as observed by optical microscopy (fig. 2).

Table 1. Comparison of the peak positions determined by the photonic band structure, approximation of the dominant wavelength, RCWA and microspectrophotometry.

Directions	Band structure	Dominant wavelength	RCWA	MSP
(111) or ΓL	577 nm	563 nm	578 nm	566 nm
(100) or ΓX	506 nm	487 nm	Not calculated	491 and 507 nm
(110) or ΓK	487 nm	459 nm	Not calculated	464 and 482 nm

3.4 Assessment of the diffraction in the visible range

In order to show how light interacts with the photonic crystals and to find out the origin of the diffusive aspect of the matt green coloration, we assess the diffraction properties of the nanostructure by considering the periodicity in the plane of the chitin layers. A reciprocal lattice vector $\vec{g}$ (norm: g) must be added to the component of the incident wavevector $\overrightarrow{k_{\parallel}}$ that is parallel to the photonic crystal surface. Taking this into account, the dominant reflected wavelength formula (at normal incidence) becomes[4]:

$$\lambda_g = \frac{2p\bar{n}}{\sqrt{m^2+\left(\frac{pg}{\pi}\right)^2}}. \quad (5)$$

The specular reflection predicted by eq. (4) corresponds to the case $g = 0$, i.e., no diffraction. The lateral periodicity therefore induces reflectance peaks (due to diffraction) at wavelengths shorter than the main peak wavelength predicted by eq. (4).

For the (111) direction, the norm of the six shortest non zero $\vec{g}$-vectors is:

$$g = \frac{2}{\sqrt{3}}\frac{2\pi}{a} \tag{6}$$

where a is equal to 280 nm.

By plugging that expansion of g into eq. (5), diffraction peaks located at 263 nm ($m = 1$) and 205 nm ($m = 2$), both below the visible range, are predicted. Higher diffraction orders (larger $\vec{g}$-vectors) give rise to λ_g values below 200 nm.

Solving Maxwell's equations using RCWA provides us with reflectance spectrum components corresponding to each reciprocal lattice vector $\vec{g}$. For the six reciprocal lattice vectors mentioned above, reflectance peaks are found at about 224 nm and 203 nm. The difference between these values and those predicted by eq. (5) is explained by the fact that eq. (5) is valid strictly at wavelengths much larger than $p = a\sqrt{2/3} = 229$ nm. These results confirm the fact that the photonic crystal does not diffract visible light (but UV light) and therefore that the matt green color is not due to diffraction. The incident light is only specularly reflected by a single photonic domain.

3.5 Polycrystalline aspects

In this section, the disorder in the photonic crystal facet orientation is discussed. The diversity of colors produced by the different photonic crystal orientations is represented on the chromaticity diagram using reflectance spectra measured by MSP (fig. 9a). However, the coloration perceived by the naked eye is an additive color, i.e., a spatial average of all these colors. Chromaticity coordinates, when they are calculated from reflectance spectra measured by SP in specular configuration (fig. 6b) with the incidence angle θ ranging from 0° to 45°, do not change very much with the angle (fig. 9b). This result is an indication that the variety of colors produced by the different photonic crystal orientations is "mixed" when it is observed in the far-field. Indeed, in the SP measurements, the illuminated area is much larger (several square millimeters) than the size of a single photonic crystal domain.

The color mixing effect was confirmed by simulations. Chromaticity coordinates, when they are calculated from simulated reflectance spectra corresponding to the (111) orientation of the photonic crystal at different incident angles (fig. 8) are scattered across the chromaticity diagram (fig. 9c). Change of the incidence angle gives rise to yellow, green and blue colors. These are the iridescent colors that can only be observed when measuring reflectance on a single photonic crystal domain, using MSP. The chromaticity coordinates calculated from the average of these reflectance spectra are plotted on fig. 9d. We insist on the fact that the result corresponds to the average of the spectra and not to the average of the x and y chromaticity coordinates. Averaging over the propagation directions (or angles) is a common method used in order to simulate the diffusive properties due to the disorder exhibited by natural structures.[4, 18] The chromaticity point in fig. 9d is located in the same region as those in fig. 9b. We remind here that the comparison of colors using the chromaticity diagram is quite complicated. The distance between two chromaticity points depends indeed on their positions on this diagram.

We note that, in the SP measurements, every crystallographic orientation contributes to the coloration while in the numerical simulations, only the (111) direction is taken into account. It would be interesting to introduce the effect of orientational disorder in our numerical simulations (i.e., other orientations should be considered). However, the study of other crystallographic directions is more complicated to perform because of the anisotropy of the unit cell of the photonic crystal. In the case of an inverse opal, the isotropy of the unit cell (one single sphere) allows to simulate the reflectance spectra for different directions.[16] It is probably useless to study the effect of disorder by a method such as ray-tracing because the orientation of the scales and the specular reflection on them do not really allow light waves to interact with several photonic crystal domains. We are currently adapting the RCWA method in order to be able to calculate the reflectance spectra independently of the orientation of the non diffracting photonic crystal with anisotropic unit cell. It could also be interesting to calculate the average of reflectance spectra for a realistic statistical distribution of incidence angles.

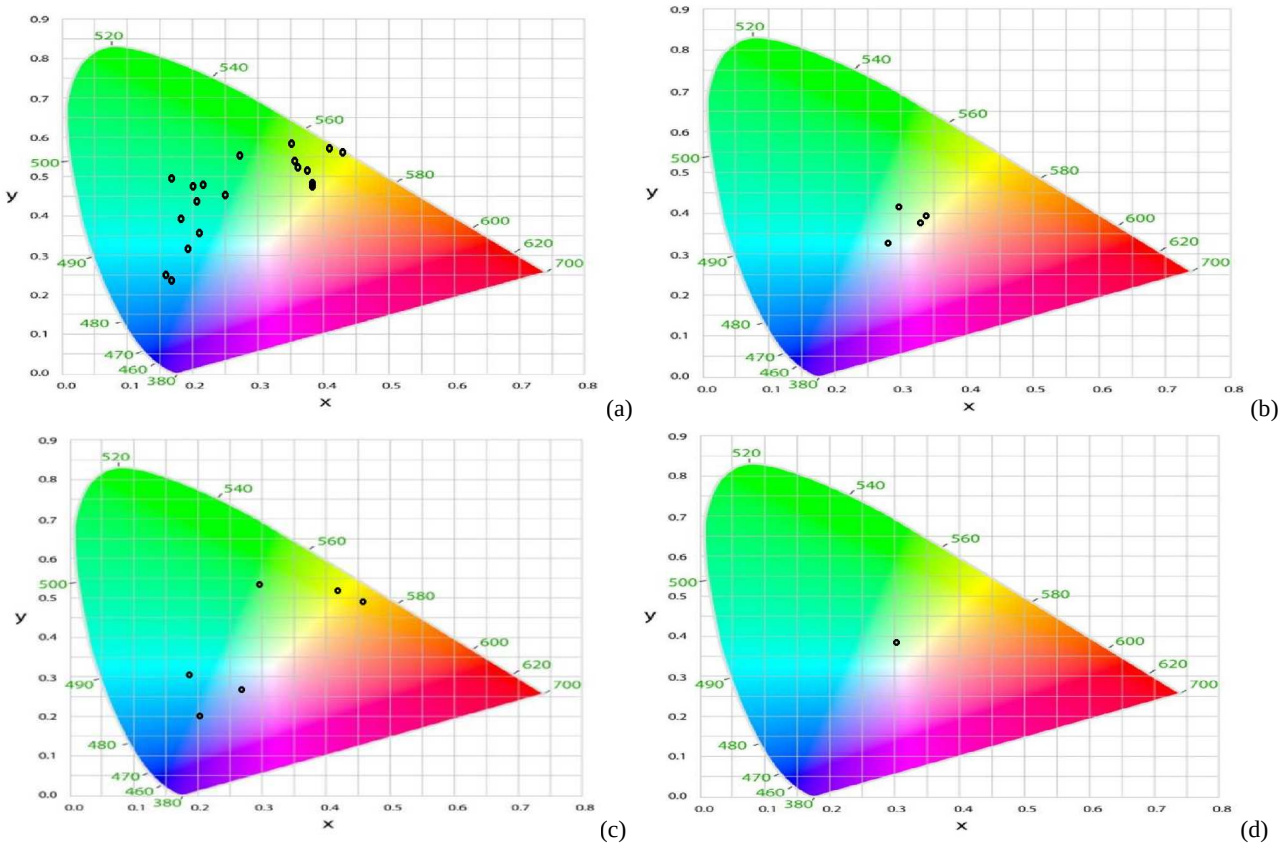

Figure 9. Chromaticity diagrams. (a) Diversity of colors produced by the interaction of light with the photonic polycrystal structure. The coordinates were calculated from reflectance spectra obtained by microspectrophotometry (fig. 6a). (b) Colors according to the incidence angle θ (ranging from 0° to 45° by step of 15°) determined from reflectance spectra measured by spectrophotometry in specular configuration (fig. 6b). (c) Colors according to the incident angle θ (ranging from 0° to 75° by step of 15°) calculated from simulated reflectance spectra corresponding to the (111) orientation of the photonic crystal (fig. 8). Color is yellow at small incidence angles and turns to blue as the angle increases. (d) Color obtained by averaging the simulated reflectance spectra of fig. 8. (colors available online)

All these results demonstrate that the additive color of the weevil is actually due to a mixing of various colors produced by different orientations of the photonic crystal present in the polycrystal structure (fig. 10). The chromaticity diagrams (fig. 9) confirm our observations by optical microscopy: the matt green coloration is due to multi-length-scale coloration phenomena. Each photonic crystal domain is iridescent, reflecting a color depending on the crystallographic orientation. However, the color is not due to this single phenomenon but rather to the interaction of light with the disordered polycrystalline structure. Each scale is composed of photonic crystal domains (several tens of micrometers in size) with different orientations and irregular interfaces between them. Furthermore, scales are juxtaposed. The optical responses of the nanoscale structures are added in such a way that the reflectance becomes independent of the observation angle: whatever the illumination conditions are, the green coloration of the beetle is almost the same. These multi-scale visual effects could serve effectively the ecological needs of the insect. Its color is certainly important since the beetle appears strongly colored from every observation direction when observed at (very) short distances. This could play a role in interspecific recognition. In the far-field, the green matt omnidirectional color is probably involved in camouflage.

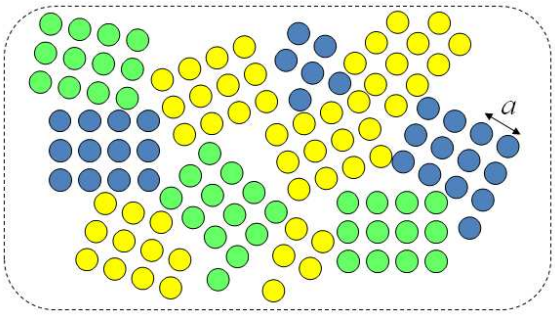

Figure 10. The different orientations of the photonic crystal exhibit various colors. This disorder leads to the loss of the iridescence by a spatial average of all these colors. (colors available online)

As in the case of *Entimus imperialis*, bright colors visible from any directions in the far-field and due to FCC three-dimensional photonic crystals were also observed on the cuticle of weevils (*Pachyrhynchus argus*[25], *Pachyrrhynchus congestus pavonius*[18] and *Eupholus magnificus*[26]), longhorn beetles (*Pseudomyagrus waterhousei*[27] and *Prosopocera lactator*[28]) and butterflies (*Cyanophrys remus*[29]). The non iridescent color in these cases were also due to spatial averaging of the colors produced by a disordered polycrystalline structure with different orientations of one single ordered photonic crystal, leading to omnidirectional colors, without iridescence. Contrasting with these cases, the ultrastructure found inside the scales of the diamond weevil is nearly a perfect three-dimensional photonic crystal: the size of the photonic crystal grains reaches about several tens of micrometers while it is only a few microns for the other insects.

4. CONCLUSION

The green coloration of the cavities found on the Brazilian diamond weevil *Entimus imperialis* is due to scales covering its cuticle. The scales display a great diversity of colors ranging from blue to orange. Inside scales, three-dimensional photonic crystals are observed, all having the same structure but exhibiting different orientations. The photonic crystal structure consists in the stacking of thin perforated chitin layers covered by cylindrical protrusions with a face-centered cubic symmetry. The photonic crystals are very regular and their size reaches several tens of micrometers. It is worth to note that a photonic crystal of that size is very difficult to produce artificially.

Comparison between microspectrophotometric measurements and band structure calculations enabled us to determine that the colors of the different photonic crystal domains are due to the non diffracting mode of interaction of light with various orientations of the photonic crystal. The matt green color of the insect is an additive photonic color, i.e., an average of all the single colors produced by individual photonic crystals. This principle is similar to the one used in impressionist paintings for which a set of small spots made thanks to brush strokes with different colors gives rise to an optical mixing of colors occurring in the eye of the spectator observing the painting at distance. In *Entimus imperialis*, there is a multi-length-scale effect: polycrystalline structures inside juxtaposed scales. The relative disorder found on the cuticle of the insect leads to the loss of iridescence effects produced by the crystals. In such a multiscale structure, a diffusive and non iridescent color can be created by light interference without diffraction in photonic crystal grains.

ACKNOWLEDGMENTS

The authors acknowledge the use of resources of the Electron Microscopy Facilities of the University of Namur (FUNDP), Belgium as well as the Interuniversity Scientific Computing Facility (iSCF) located at the University of Namur and supported by the Belgian National Fund for Scientific Research (F.R.S.-FNRS) under convention No. 2.4617.07. S.M., J.-F.C. and C.V. were also supported by the F.R.S.-FNRS as Research Fellow, Research Associate and Postdoctoral Researcher, respectively.

REFERENCES

[1] Kinoshita, S., [Structural Colors in the Realm of Nature], World Scientific Publishing Co, Singapore (2008).
[2] Berthier, S., [Photonique des Morphos], Springer, Paris (2010).
[3] Vigneron, J.-P., Pasteels, J. M., Windsor, D. M., Vértesy, Z., Rassart, M., Seldrum, T., Dumont, J., Deparis, O., Lousse, V., Biró, L. P., Ertz, D. and Welch, V. L., "Switchable reflector in the Panamian tortoise beetle *Charidotella egregia* (Chrysomelidae: Cassidinae)," Phys. Rev. E 76, 031907 (2007).
[4] Rassart, M., Colomer, J.-F., Tabarant, T. and Vigneron, J.-P., "Diffractive hygrochromic effect in the cuticle of the hercules beetle *Dynastes hercules*," New J. Phys. 10, 033014 (2008).
[5] Rassart, M., Simonis, P., Bay, A., Deparis, O. and Vigneron, J.-P., "Scales coloration change following water absorption in the beetle *Hoplia coerulea* (Coleoptera)," Phys. Rev. E 80, 031910 (2009).
[6] Liu, F., Dong, B. Q., Liu, X. H., Zheng, Y. M. and Zi, J., "Structural color change in longhorn beetles *Tmesisternus isabellae*," Opt. Express 17(18), 16183-16191 (2009).
[7] Eliason, C. H. and Shawkey, M. D., "Rapid, reversible response of iridescent feather color to ambient humidity," Opt. Express 18(20), 21284 (2010).
[8] Shawkey, M. D., D'Alba, L., Wozny, J., Eliason, C., Koop, J. A. H. and Jia, L., "Structural color change following hydration and dehydration of iridescent mourning dove (*Zenaida macroura*) feathers," Zoology 114, 59-68 (2011).
[9] Potyrailo, R. A., Ghiradella, H., Vertiatchikh, A., Dovidenko, K., Cournoyer, J. R. and Olson, E., "*Morpho* butterfly wing scales demonstrate highly selective vapour response," Nat. Photonics 1, 123-128 (2007).
[10] Biró, L. P., Kertész, K., Vértesy, Z. and Bálint, Zs., "Photonic nanoarchitectures occurring in butterfly scales as selective gas/vapor sensors," Proc. SPIE 7057, 705706 (2008).
[11] Mouchet, S., Deparis, O. and Vigneron, J.-P., "Unexplained high sensitivity of the reflectance of porous natural photonic structures to the presence of gases and vapours in the atmosphere," Proc. SPIE 8424, 842425 (2012), doi: 10.1117/12.921784.
[12] Deparis, O., Khuzayim, N., Parker, A. and Vigneron, J.-P., "Assessment of the antireflection property of moth wings by three-dimensional transfer-matrix optical simulations," Phys. Rev. E 79, 041910 (2009).
[13] Herman, A., Vandenbem, C., Deparis, O., Simonis, P. and Vigneron, J.-P., "Nanoarchitecture in the black wings of *Troides magellanus*: a natural case of absorption enhancement in photonic materials," Proc. SPIE 8094, 80940H (2011).
[14] Deparis, O. and Vigneron, J.-P., "Modeling the photonic response of biological nanostructures using the concept of stratified medium: The case of a natural three-dimensional photonic crystal," Mater. Sci. Eng. B-Adv. 169, 12-15 (2010).
[15] Moharam, M. G. and Gaylord, T. K., "Rigorous coupled-wave analysis of planar-grating diffraction," J. Opt. Soc. Am. 71(7), 811-818 (1981).
[16] Vigneron, J.-P. and Lousse V., "Variation of a photonic crystal color with the Miller indices of the exposed surface," Proc. of SPIE 6128, 61281G-1 (2006).
[17] Deparis, O., Vandenbem, C., Rassart, M., Welch, V. L. and Vigneron, J.-P., "Color-selecting reflectors inspired from biological periodic multilayer structures," Opt. Express 14(8), 3547-3555 (2006).
[18] Welch, V. L., Lousse, V., Deparis, O., Parker, A. R. and Vigneron, J.-P., "Orange reflection from a three-dimensional photonic crystal in the scales of the weevil *Pachyrrhynchus congestus pavonius* (Curculionidae)," Phys. Rev. E 75, 041919 (2007).
[19] Johnson, S. G. and Joannopoulos, J. D., "Block-iterative frequency-domain methods for Maxwell's equations in a planewave basis," Opt. Express 8(3), 173-190 (2001).
[20] Judd, D. B. and Wyszecki, G., [Color in Business, Science and Industry], John Wiley & Sons, New York (1975).
[21] Chamberlin, G. J. and Chamberlin, D. G., [Colour: Its Measurement, Computation and Application], Heyden international topics in science, London, (1980).
[22] Vigneron, J.-P., Ouedraogo, M., Colomer, J.-F. and Rassart, M., "Spectral sideband produced by a hemispherical concave multilayer on the African shield-bug *Calidea panaethiopica* (Scutelleridae)," Phys. Rev. E 79, 021907 (2009).
[23] Stavenga, D. G., Wilts, B. D. and Leertouwer, H. L., "Polarized iridescence of the multilayered elytra of the Japanese Jewel beetle, *Chrysochroa fulgidissima*," Philos. T. R. Soc. B 366, 709-723 (2011).
[24] Sollas, I. B. J., "On the Identification of Chitin by Its Physical Constants," Proc. R. Soc. Lond. B 79, 474-484 (1907).
[25] Parker, A. R., Welch V. L., Driver D. and Martini N., "Opal analogue discovered in a weevil," Nature 426, 786-787 (2003).
[26] Pouya, C., Stavenga, D. G. and Vukusic, P., "Discovery of ordered and quasi-ordered photonic crystal structures in the scales of the beetle *Eupholus magnificus*," Opt. Express 19(12), 11355-11364 (2011).

[27] Simonis, P. and Vigneron, J.-P., "Structural color produced by a three-dimensional photonic polycrystal in the scales of a longhorn beetle: *Pseudomyagrus waterhousei* (Coleoptera: Cerambicidae)," Phys. Rev. E 83, 011908 (2011).
[28] Colomer, J.-F., Simonis, P., Bay, A., Cloetens, P., Suhonen, H., Rassart, M., Vandenbem, C. and Vigneron J.-P., "Photonic polycrystal in the greenish-white scales of the African longhorn beetle *Prosopocera lactator* (Cerambycidae)," Phys. Rev. E 85, 011907 (2012).
[29] Kertész, K., Bálint, Zs., Vértesy, Z., Márk, G. I., Lousse, V. and Vigneron, J.-P., "Gleaming and dull surface textures from photonic-crystal-type nanostructures in the butterfly *Cyanophrys remus*," Phys. Rev. E 74, 021922 (2006).